Journal of Mechanical Engineering Research Vol. 2(2), pp. 39-51, March 2010
Available online at http://www.academicjournals.org/jmer

Full Length Research Paper

Geometrically nonlinear transient analysis of functionally graded shell panels using a higher-order finite element formulation

S. Pradyumna[1]* Namita Nanda[1] and J. N. Bandyopadhyay[2]

[1]Department of Civil Engineering, National Institute of Technology Rourkela, Orissa, India 769008.
[2]Department of Civil Engineering, Indian Institute of Technology, Kharagpur, West Bengal, India 721302.

Accepted 29 November, 2009

Nonlinear transient analysis of functionally graded curved panels is carried out employing a higher-order C^0 finite element formulation. The element consists of nine degrees-of-freedom per node with higher-order terms in the Taylor's series expansion which represents the higher-order transverse cross sectional deformation modes. The formulation includes Sanders' approximation for doubly curved shells considering the effects of rotary inertia, transverse shear and moderately large rotations in the von Kárman sense. A realistic parabolic distribution of transverse shear strains through the shell thickness is assumed and the use of shear correction factor is avoided. The accuracy of the formulation is validated by comparing the results with those available in the literature. The transient dynamic responses of the functionally graded shell panels are investigated by varying the volume fraction index using a simple power law distribution. Material properties are assumed to be temperature-independent and graded in the thickness direction according to a simple power law distribution in terms of the volume fractions of the constituents. Heat conduction between ceramic and metal constituents is neglected. Effects of different panel geometry parameters, boundary conditions and loadings are studied.

Key words: Functionally graded materials, higher-order formulation, geometric nonlinearity, transient analysis.

INTRODUCTION

Functionally graded materials (FGMs) are heterogeneous composite materials usually made from a mixture of metals and ceramics. The material properties of FGM are graded but continuous and are controlled by the variation of the volume fraction of the constituent materials. The concept of FGM was first proposed by Koizumi (1993). Functionally graded materials have the advantage of their ability to withstand high temperature gradients unlike fibre matrix composites, which show mismatch of mechanical properties across an interface of two discrete materials bonded together and resulting in debonding at high temperatures in some cases.

In FGMs, the ceramic material provides high temperature resistance due to its low thermal conductivity while the ductile metal component provides structural strength and fracture toughness.

Functionally graded materials are now being strongly considered as a potential structural material for future high-speed spacecraft. They are widely applied where the operating conditions are severe, for example, wear resistant linings for handling large heavy abrasive exchanger tubes, thermoelastic generators, heat engine components etc. FGMs can also be used to eliminate or control the thermal deformation (Wetherhold et al., 1996).

Nonlinear dynamic responses of composite plates and shells were studied by many researchers including Nath et al. (1985), Civalek and Ülker (2005), Civalek (2006). Intensive researches were reported in the available literature on the analysis of FGM. Elastic problem of thick walled functionally graded (FG) tubes was studied by Fukui and Yamanaka (1992). Fuchiyama and Noda (1995) investigated the transient heat transfer and transient thermal stresses in FG plates using the FEM.

*Corresponding author. E-mail: spradyumna@nitrkl.ac.in. Tel: +91-661-2462309

Praveen and Reddy (1998) investigated the nonlinear transient thermoelastic behavior of functionally graded ceramic-metal plates and found that, in general, the response of plates with material properties between those of ceramic and metal is not intermediate to the responses of the ceramic and metal plates. Pseudo-dynamic thermoelastic response of FG ceramic-metal cylinders was studied by Praveen et al. (1999) using the finite element method. Aboudi et al. (1999) developed a Cartesian co-ordinate based higher-order theory for FGMs, which circumvents the problematic use of the standard micromechanical approach, based on the concept of a representative volume element, commonly employed in FG composites. Reddy (2000) obtained Navier's solutions and finite element results based on the third-order shear deformation theory for functionally graded plates.

Woo and Meguid (2001) carried out nonlinear analysis of FG plates and shallow shells subjected to transverse mechanical load and a temperature field. Nonlinear bending response of FG plates subjected to transverse loads in thermal environments was investigated by Shen (2002) employing a mixed Galerkin-perturbation technique. Bhangale and Ganesan (2006) carried out static analysis of simply supported functionally graded and layered magneto-electro-elastic plates. Large deflection behavior of FG plates under pressure loads was investtigated by GhannadPour and Alinia (2006). Panda and Ray (2006) and Ray and Sachade (2006) analysed the FG plates integrated with the piezoelectric fiber-reinforced composite layer.

Many researchers studied dynamic behavior of FG structures in the past few years. Loy et al. (1999) investigated the free vibration of simply supported FG cylindrical shells. Pradhan et al. (2000) studied the effect of different boundary conditions on the natural frequencies of FG cylindrical shells made up of stainless steel and zirconia. Influence of the volume fractions and the effects of configurations of the constituent materials on the parametric instability regions of FG plates were investigated by Ng et al. (2000). Han et al. (2002) pro-posed a numerical method for analyzing transient waves in FG cylindrical shells excited by impact point loads. Yang and Shen (2002) investigated the free and forced vibration characteristics of shear deformable initially stressed FG plates in thermal environment.

By considering the material properties of the constituents to be nonlinear functions of the temperature and graded in the thickness direction by power law distribution, Yang and Shen (2003) investigated the free vibration and parametric resonance of shear deformable FG cylindrical panels. Yang et al. (2003) presented a large amplitude vibration analysis of pre-stressed FGM laminated plates composed of a shear deformable FG layer and two surface-mounted piezoelectric actuator layers. Patel et al. (2005) carried out the free vibration analysis of FG elliptical and cylindrical shells using a higher-order theory. Nonlinear free vibration behavior of FG plates is investigated by Woo et al. (2006). Huang and shen (2004) studied the nonlinear vibrations and dynamic response of FG rectangular plates in thermal environments.

A semi-analytical method was developed by Allahverdizadeh et al. (2008) for nonlinear free and forced axisymmetric vibration of a thin circular FG plate. A considerable amount of work was done on the development of higher-order theories to study the static, dynamic and stability behavior of plates and shells. Many researchers developed higher-order theories in which the displacements of the middle surface would expand as cubic functions of the thickness co-ordinate and the transverse displacement was assumed to be constant through the thickness.

This displacement field led to the parabolic distribution of the transverse shear stresses and, therefore, the use of shear correction factors could be avoided. To the best of the authors' knowledge, however, limited literature is available related to the application of higher-order theory for studying the nonlinear transient behavior of FG curved panels and the authors attempt to fill this lacuna is first of its kind and new.

Therefore, the geometric nonlinear transient analysis of FG curved panels is studied herein by using the higher-order shear deformation theory (HSDT) developed by Kant and Khare (1997) and including the twist curvature while employing the finite element method. The nonlinearity used in the formulation is due to von Kárman. Material properties are assumed to be temperature-independent and heat conduction between ceramic and metal constituents is neglected.

Mathematical formulation

Let us consider a shell element made of a FG material with the co-ordinate system (*x,y z*) shown in Figure 1, and chosen such that the plane *x-y* at *z* = 0 coincides with the mid-plane. In order to approximate the three-dimensional elasticity problem to a two-dimensional one, the displacement components *u(x,y,z)*, *v(x,y,z)* and *w(x,y,z)* at any point in the shell space are expanded in Taylor's series in terms of the thickness co-ordinates. The elasticity solution indicates that the transverse shear stresses vary parabolically through the element thickness. This requires the use of a displacement field in which the in-plane displacements are expanded as cubic functions of the thickness co-ordinate. The displacement fields, which satisfy the above criteria are assumed in the form as given by Kant and Khare (1997).

$$u(x,y,z) = u_0(x,y) + z\theta_y + z^2 u_0^*(x,y) + z^3\theta_y^*(x,y)$$
$$v(x,y,z) = v_0(x,y) - z\theta_x + z^2 v_0^*(x,y) - z^3\theta_x^*(x,y)$$
$$w(x,y,z) = w_0 \qquad (1)$$

Where *u, v* and *w* are the displacements of a general point (*x,y,z*) in an element of the laminate along *x, y* and *z* directions, respectively. The parameters u_0, v_0, w_0, θ_x and θ_y are the displacements and

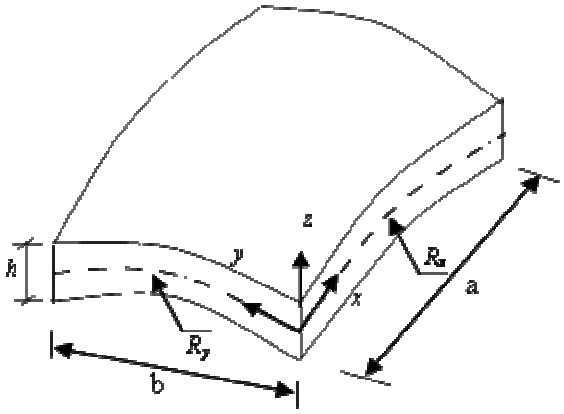

Figure 1. Spherical Shell panel and coordinate system.

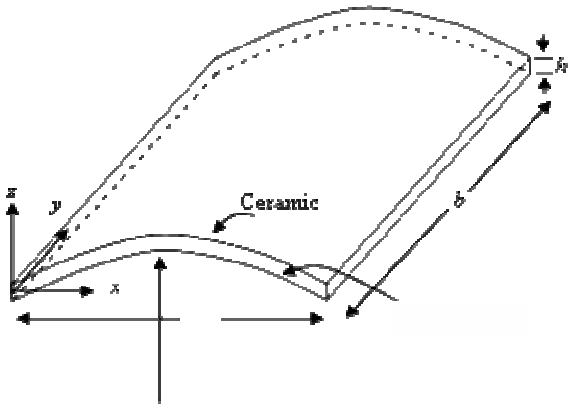

Figure 2. Cylindrical FG Shell panel.

rotations of the middle plane, while $u_0^*,\ v_0^*,\ \theta_x^*$ and θ_y^* are the higher-order displacement parameters at the mid-plane.

The present theory includes large displacements in the sense of von Kárman, which in particular imply that the first order derivatives of the tangential displacement components with respect to *x, y* and *z* are small so that their particular products can be neglected.

The strain-displacement relations are as follows: (Reddy,1984 and Chandrashekhara, 1989)

$$\varepsilon_x = \frac{\partial u}{\partial x} + \frac{w}{R_x} + \frac{1}{2}\left(\frac{\partial w}{\partial x}\right)^2 \qquad \varepsilon_y = \frac{\partial v}{\partial y} + \frac{w}{R_y} + \frac{1}{2}\left(\frac{\partial w}{\partial y}\right)^2,$$

$$\gamma_{xy} = \frac{\partial v}{\partial x} + \frac{\partial u}{\partial y} + \frac{2w}{R_{xy}} + \frac{\partial w}{\partial x}\frac{\partial w}{\partial y},$$

$$\gamma_{xz} = \frac{\partial u}{\partial z} + \frac{\partial w}{\partial x} - C_1\frac{u}{R_x} - C_1\frac{v}{R_{xy}},$$

$$\gamma_{yz} = \frac{\partial v}{\partial z} + \frac{\partial w}{\partial y} - C_1\frac{v}{R_y} - C_1\frac{u}{R_{xy}} \qquad (2)$$

Where R_x and R_y are the radii of curvature of the shell along *x* and *y* directions, respectively, and R_{xy} is the twist radius of curvature.

Substituting Equation in Equation, linear strain terms are written as,

$$\varepsilon_{xL} = \varepsilon_{x0} + z\kappa_x + z^2\varepsilon_{x0}^* + z^3\kappa_x^*$$
$$\varepsilon_{yL} = \varepsilon_{y0} + z\kappa_y + z^2\varepsilon_{y0}^* + z^3\kappa_y^*$$
$$\gamma_{xyL} = \gamma_{xy0} + z\kappa_{xy} + z^2\gamma_{xy0}^* + z^3\kappa_{xy}^*$$
$$\gamma_{xz} = \varphi_x + z\kappa_{xz} + z^2\varphi_x^* + z^3\kappa_{xz}^*$$
$$\gamma_{yz} = \varphi_y + z\kappa_{yz} + z^2\varphi_y^* + z^3\kappa_{yz}^* \qquad (3)$$

Where,

$$\{\varepsilon_{x0},\varepsilon_{y0},\gamma_{xy0},\varepsilon_{x0}^*,\varepsilon_{y0}^*,\gamma_{xy0}^*\} = \left\{\frac{\partial u_0}{\partial x}+\frac{w_0}{R_x},\frac{\partial v_0}{\partial y}+\frac{w_0}{R_y},\frac{\partial u_0}{\partial y}+\frac{\partial v_0}{\partial x}+\frac{2w_0}{R_{xy}},\frac{\partial u_0^*}{\partial x},\frac{\partial v_0^*}{\partial y},\frac{\partial v_0^*}{\partial x}+\frac{\partial u_0^*}{\partial y}\right\}$$

$$\{\kappa_x,\kappa_y,\kappa_{xy},\kappa_x^*,\kappa_y^*,\kappa_{xy}^*\} = \left\{\frac{\partial\theta_y}{\partial x},-\frac{\partial\theta_x}{\partial y},\frac{\partial\theta_y}{\partial y}-\frac{\partial\theta_x}{\partial x}+C_0\frac{\partial u_0}{\partial y}-C_0\frac{\partial v_0}{\partial x},\frac{\partial\theta_y^*}{\partial x},-\frac{\partial\theta_x^*}{\partial y},\frac{\partial\theta_y^*}{\partial y}-\frac{\partial\theta_x^*}{\partial x}\right\}$$

$$\{\varphi_x,\varphi_y\} = \left\{\frac{\partial w_0}{\partial x}+\theta_y - C_1\frac{u_0}{R_x} - C_1\frac{v_0}{R_{xy}},\frac{\partial w}{\partial y}-\theta_x - C_1\frac{v_0}{R_{y\,1}} - C_1\frac{u_0}{R_{xy}}\right\}$$

$$\{\varphi_x^*,\varphi_y^*\} = \left\{3\theta_y^* - C_1\frac{u_0^*}{R_x} - C_1\frac{v_0^*}{R_{xy}},-3\theta_x^* - C_1\frac{v_0^*}{R_y} - C_1\frac{u_0^*}{R_{xy}}\right\}$$

$$\{\kappa_{xz},\kappa_{yz},\kappa_{xz}^*,\kappa_{yz}^*\} = \left\{2u_o^* - C_1\frac{\theta_y}{R_x} + C_1\frac{\theta_x}{R_{xy}},2v_o^* + C_1\frac{\theta_x}{R_y} - C_1\frac{\theta_y}{R_{xy}},-C_1\frac{\theta_y^*}{R_x} + C_1\frac{\theta_x^*}{R_{xy}},C_1\frac{\theta_x^*}{R_x} - C_1\frac{\theta_y^*}{R_{xy}}\right\}$$

(4)

C_1 is a tracer by which the analysis can be reduced to that of shear deformable Love's first approximation and $C_0 = 0.5(1/R_x - 1/R_y)$ is the result of Sanders' theory which accounts for the condition of zero strain for rigid body motion.

FG material properties

The panels considered (Figures 1 and 2) in the present analysis are assumed to be of uniform thickness *h*. It is also assumed that the panel is made from a mixture of ceramic and metals and the material composition is continuously varied such that the top surface ($z = h/2$) of the panel is ceramic rich, whereas the bottom surface ($z = -h/2$) is metal rich. Thus, the effective material property *P* (such as Young's modulus, Poisson's ratio, mass density etc.) can be expressed as

$$P = \sum_{j=1}^{k} P_j V_j \qquad (5)$$

Where P_j and V_j are the material property and volume fraction of

the constituent material *j*, respectively, satisfying the volume fraction of all the constituent materials as,

$$\sum_{j=1}^{k} V_j = 1 \quad (6)$$

For a panel with the reference surface at its middle surface, the volume fraction can be written as

$$V_j = \left(\frac{2z+h}{2h}\right)^n \quad (7)$$

In which, *n* characterizes the material variation through the panel thickness, which is referred to as volume fraction index and $0 \le n \le \infty$.
Material properties for a FG solid with two constituent materials are given by,

$$P(z) = (P_c - P_m)\left(\frac{2z+h}{2h}\right)^n + P_m \quad (8)$$

Where P_c and P_m refer to the corresponding properties of the ceramic and metal constituents, respectively. By using these material properties, the stresses can be determined as,

$$\begin{Bmatrix}\sigma_x\\ \sigma_y\\ \tau_{xy}\\ \tau_{yz}\\ \tau_{xz}\end{Bmatrix} = \begin{bmatrix} Q_{11} & Q_{12} & 0 & 0 & 0\\ Q_{12} & Q_{22} & 0 & 0 & 0\\ 0 & 0 & Q_{66} & 0 & 0\\ 0 & 0 & 0 & Q_{44} & 0\\ 0 & 0 & 0 & 0 & Q_{55}\end{bmatrix} \begin{Bmatrix}\varepsilon_x\\ \varepsilon_y\\ \gamma_{xy}\\ \gamma_{yz}\\ \gamma_{xz}\end{Bmatrix} \quad (9)$$

Where $Q_{11} = Q_{22} = \frac{E(z)}{1-\nu^2}$; $Q_{12} = \frac{\nu E(z)}{1-\nu^2}$;

$$Q_{44} = Q_{55} = Q_{66} = G(z) = \frac{E(z)}{2(1+\nu)} \quad (10)$$

Equation can also be written as,

$$\{\sigma\} = [\overline{Q}]\{\varepsilon\} \quad (11)$$

Where $[\overline{Q}]$ is effective stiffness coefficient matrix given by the relation,

$$[\overline{Q}] = (Q_c - Q_m)\left(\frac{2z+h}{2h}\right)^n + Q_m \quad (12)$$

Q_c and Q_m are the effective stiffness coefficient matrices for ceramic and metal constituents, respectively.

Finite element formulation

In the present study, an eight-noded C^o element is employed with nine degrees of freedom viz., $u_0, v_0, w_0, \theta_x, \theta_y, u_0^*, v_0^*, \theta_x^*$ and θ_y^* at each node. The displacement fields $\{u\}$ at any point on the mid-surface is given by

$$\{u\} = [N]\{d\} \quad (13)$$

Where $[N]$ and $\{d\}$ are the interpolating function and displacement vector, respectively, associated with node i.
The virtual work equation for nonlinear dynamic equilibrium in Lagrangian co-ordinate system at time $t+\Delta t$ may be written (Bathe et al., 1975) as

$$\int_A \left\{\delta\, {}^{t+\Delta t}_{0}d\right\}^T [\rho] \left\{{}^{t+\Delta t}_{0}\ddot{d}\right\}^0 dA + \int_A \left\{\delta\, {}^{t+\Delta t}_{0}\varepsilon\right\}^T [\rho] \left\{{}^{t+\Delta t}_{0}s\right\}^0 dA \quad (14)$$

Where $\{d\}^T$ is the generalised displacement, δ denotes its variation, $[\rho]$ is the mass matrix and {*s*} is the stress vector.
The generalised vectors of the mid-surface strain ε can be separated into linear $\{\varepsilon_L\}$ and nonlinear $\{\varepsilon_{NL}\}$ parts as given by

$$\{\varepsilon\} = \{\varepsilon_L\} + \{\varepsilon_{NL}\} = \left([B_L] + \frac{1}{2}[B_{NL}]\right)\{d\} \quad (16)$$

In Equation, $[B_L]$ is the linear strain-displacement matrix and $[B_{NL}]$ is the nonlinear strain-displacement matrix.
The governing equilibrium equation in the finite element form is written as (Naidu and Sinha, 2006)

$$[M_e]\{\ddot{d}\} + ([k_L] + [k_{NL}])\{d\} = \{{}^{t+\Delta t}R\} - \{{}^{t}F\}$$

Where $\{R\}$ is the external force vector and $\{F\}$ is the internal nodal force vector,

$$[M_e] = \int_A [N]^T [m][N] dA \quad (17)$$

And

$$[k_L] = \int_A [B]^T [D][B] dA \quad (18)$$

in which $[B] = [B_L] + [B_{NL}]$

$$[k_{NL}] = \int_A [G]^T [S][G] dA \quad (19)$$

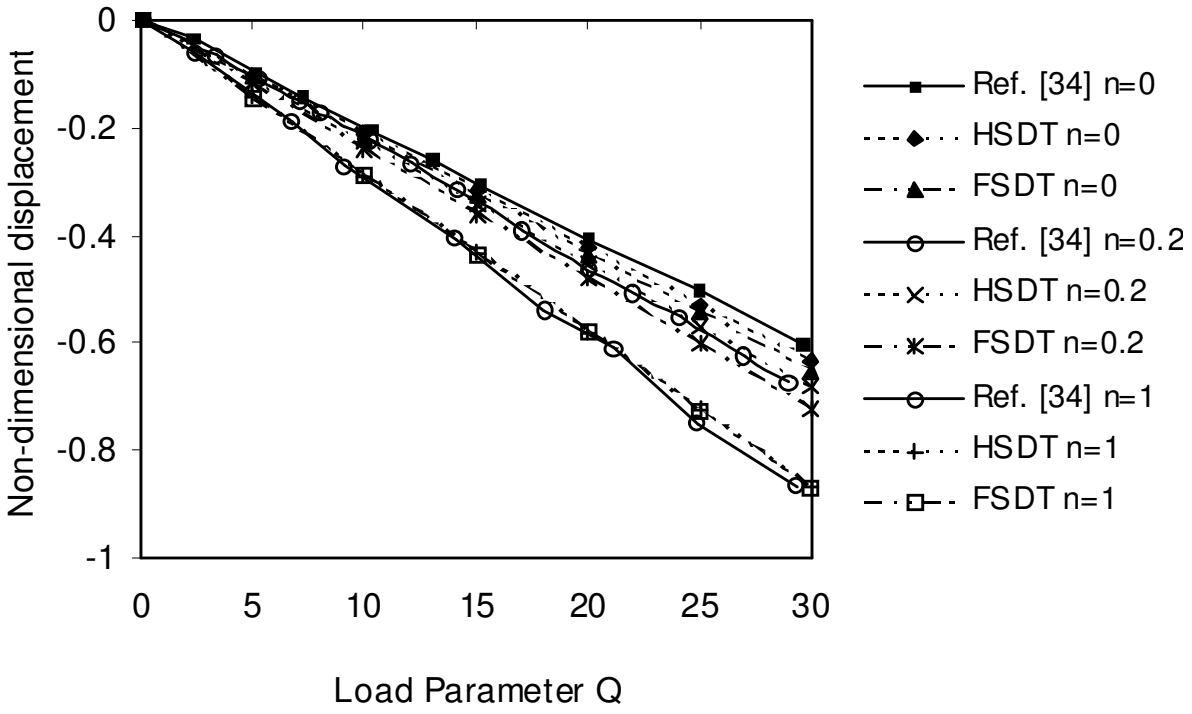

Figure 3. Load-displacement variation of SS plates for different values of *n*.

$$\{{}^{t}F\} = \int_{A} [B]\{s\}dA \qquad 20$$

$$\{{}^{t+\Delta t}R\} = \int_{A} [N]\{q_0\}dA \qquad 21$$

And

In which $\{q_0\}$ is the external applied load.
In the above equations, [*S*] is the matrix of second Piola-Kirchoff stresses, $[k_L]$ and $[k_{NL}]$ are elastic and stress stiffness matrices of an element, respectively, [*m*] is the inertia matrix and {*s*} is the stress vector of an element given by,

$$\{s\} = [D]\left(\{\varepsilon_L\} + \{\varepsilon_{NL}\}\right) \qquad 22$$

Solution procedure

The transient response of the system is calculated by using the Newmark method (Bathe et al., 1975). The solution of nonlinear equilibrium equation, Equation (16) is implemented through an incremental iterative procedure. Equation (16) can be written as,

$$\left(\left[{}^{t}K_L\right] + \left[{}^{t}K_{NL}\right]\right)\{\Delta u\}^{i} = {}^{t+\Delta t}R - {}^{t+\Delta t}F^{(i-1)} - [M]\left\{{}^{t+\Delta t}\ddot{u}\right\}^{i}$$

And

$$\{{}^{t+\Delta t}u\}^{i} = \{{}^{t+\Delta t}u\}^{(i-1)} + \{\Delta u\}$$

The index *i* indicates the number of iteration step.
In the present study, the modified Newton-Raphson iterations are applied to achieve the equilibrium at the end of each time step.

Boundary conditions

The following two boundary conditions are used in the present analysis:
(i) Simply supported boundary (SS):

$$v_0 = w_0 = \theta_y = v_0^* = \theta_y^* = 0, \quad \text{at } x = 0,\ a;$$

$$u_0 = w_0 = \theta_x = u_0^* = \theta_x^* = 0, \quad \text{at } y = 0,\ b.$$

(ii) Clamped boundary (CC):

$$u_0 = v_0 = w_0 = \theta_x = \theta_y = u_0^* = v_0^* = \theta_x^* = \theta_y^* = 0, \quad \text{at}$$

$x = 0$, a and $y = 0$, b.

RESULTS AND DISCUSSION

Comparison studies

In order to establish the correctness of the present formulation, the results obtained herein are compared with those available in the existing literature.

First, linear static analysis of a simply supported square plate of Aluminum-Zirconia with a = 0.2m and thickness 0.01m is carried out. This problem was earlier solved by Reddy (2003). The Young's modulus, Poisson's ratio and density of Aluminum are 70 GPa, 0.3 and 2707 kg/m^3, respectively and the same for Zirconia are 151 GPa, 0.3 and 3000 kg/m^3, respectively. The plate is subjected to a uniformly distributed transverse load q_0. The non-dimensional load parameter is $Q = q_0 (a/h)^4 / E_m$

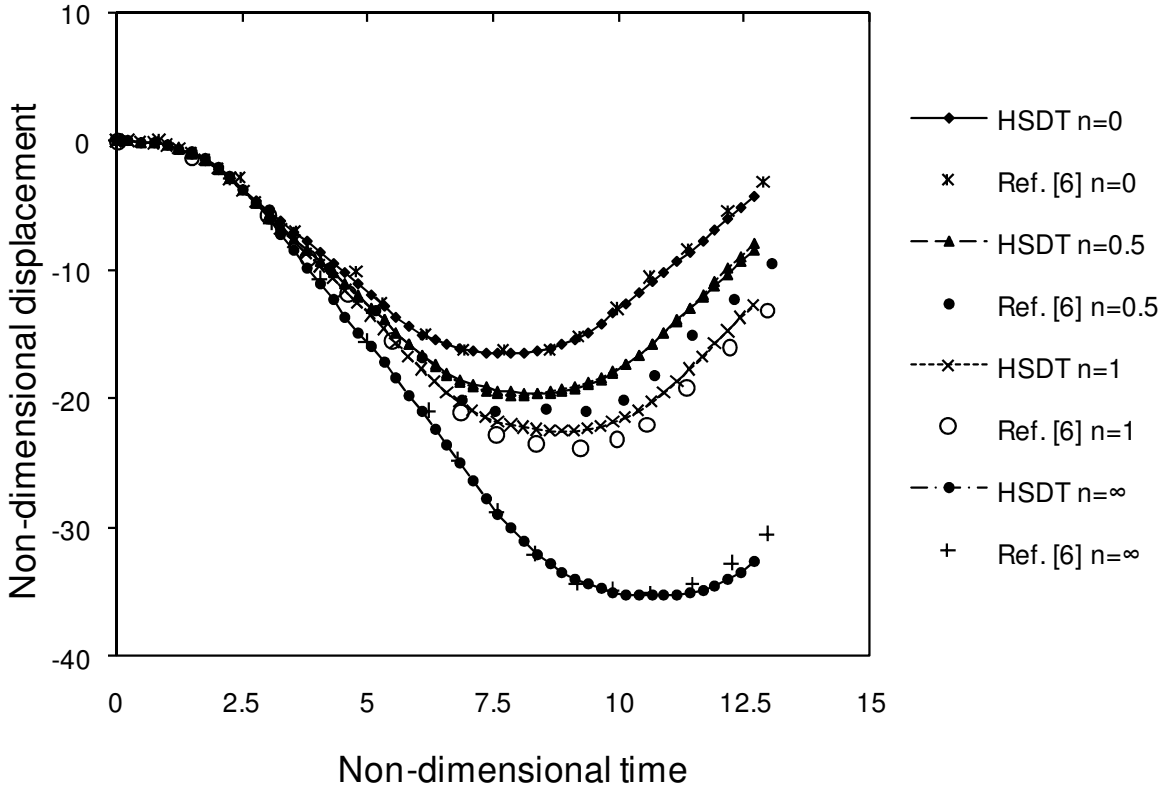

Figure 4. Comparison of transient response of a SS square plate.

and the non-dimensional displacement parameter is $\bar{w} = w/h$. The results obtained by the present formulation are compared with those of Reddy (2003) and also with the FSDT results of the authors. Figure 3 shows the variation of non-dimensional response of FGM shell panels. The material of the FG shell panels considered in the present study is Aluminum-Zirconia. The Young's modulus, Poisson's ratio and density for Aluminum are: 70 GPa, 0.3 and 2707 kg/m^3, respectively and the same for Zirconia are: 151 GPa, 0.3 and 3000 kg/m^3, respectively. The center displacement and the time are expressed in the non-dimensional form as $\bar{w} = wE_m h/(q_0 a^2)$ and $\bar{t} = t\sqrt{Em/(a^2\rho_m)}$, respectively. The values of displacement and velocity at the initial conditions are assumed as zero for obtaining the nonlinear dynamic response. The values of constants δ and α in the Newmark's integration are taken as 0.5 displacements for various load parameters and volume fraction index *n*. The present HSDT results are observed to be lower than those of the FSDT. It is evident from Figure 3 that the results obtained using FSDT are agreeing well with those of Reddy (2003).

Thereafter, a simply supported square plate is considered with the geometrical and elastic properties as specified in the earlier problem for carrying out nonlinear transient analysis. This problem was solved earlier by Praveen and Reddy (1998). The FGM plate is subjected to a uniformly distributed load of -10^6 N/m^2 and time step considered is 0.00001 s. Due to the biaxial symmetry, only one quarter of the plate is modeled for the analysis. A 2 × 2 uniform mesh is used in the quarter plate model. The non-dimensional center displacement parameter is $\bar{w} = wE_m h/(q_0 a^2)$ while the non-dimensional time is $\bar{t} = t\sqrt{Em/(a^2\rho_m)}$. Figure 4 shows the transient non-dimensional displacement vs. non-dimensional time graph for different values of volume fraction index *n*. The results are compared with those of Praveen and Reddy (1998) and found to be in good agreement.

Numerical results for the transient response of FGM shell panels

In this section, we use the above formulation to investigate the effect of various parameters like curvature (*R*/*a*), volume fraction index *n*, side to thickness ratio (*a*/*h*), aspect ratio ($\beta = a/b$), boundary conditions (clamped and simply supported) and loading types (uniformly distributed and sinusoidal) on the transient and 0.25, respectively. The time step selected, based on the convergence study, is 1 ms.

Figures 5 and 6 show the effect of curvature on the

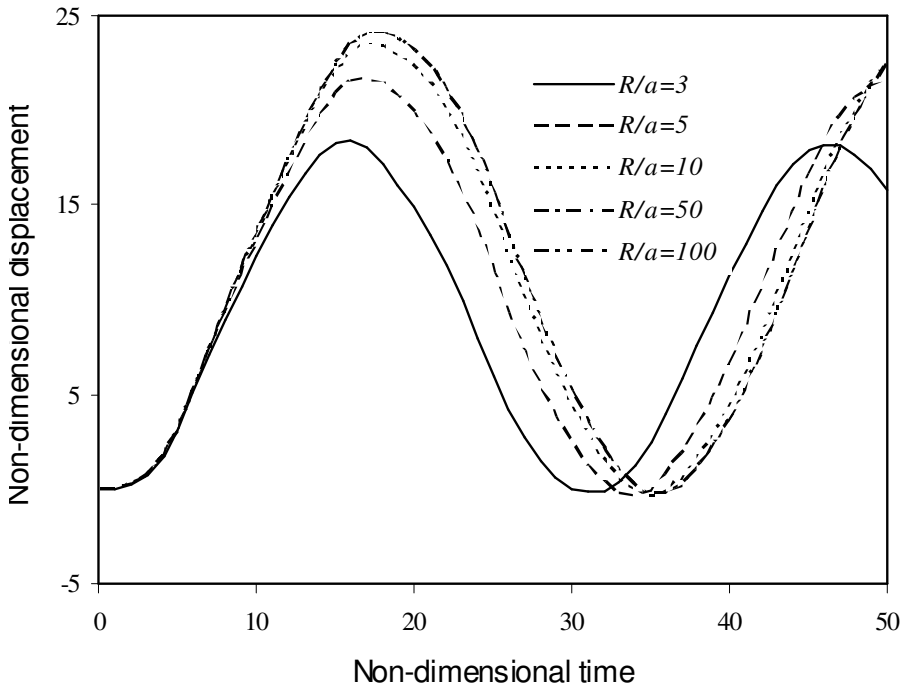

Figure 5. Effect of curvature on the transient response of SS-FG cylindrical panels ($R_x = R, R_y = \infty$).

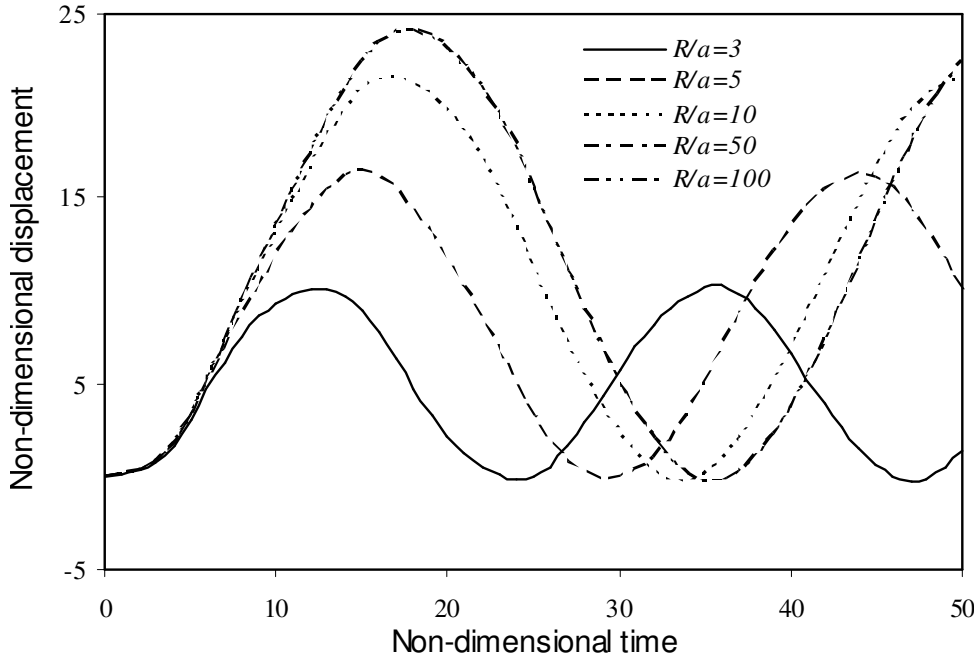

Figure 6. Effect of curvature on the transient response of SS-FG spherical panels

transient response of simply supported FGM cylindrical ($R_x = R, R_y = \infty$) and spherical ($R_x = R_y = R$) shell panels subjected to uniformly distributed load, respectively. Other parameters are kept constant and are given as $n = 1$, $a/b = 1$, and $a/h = 20$. It is observed from Figures 5 and 6 that the transient displacements increase

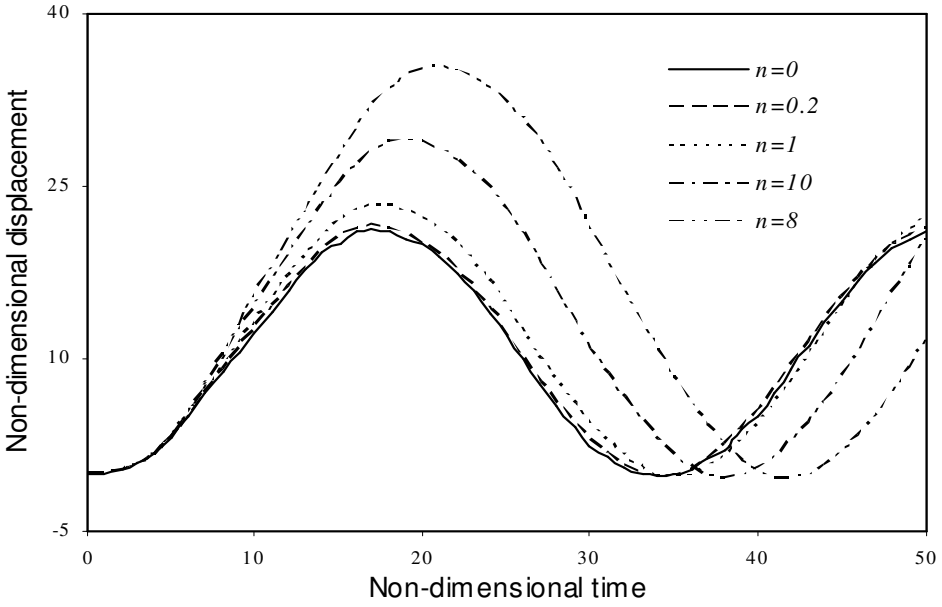

Figure 7. Effect of volume fraction index *n* on the transient response of SS-FG cylindrical panels.

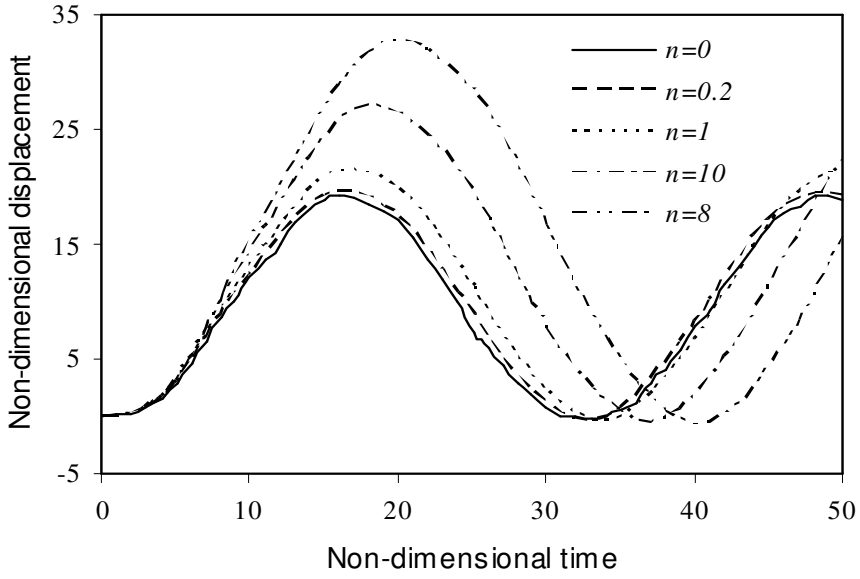

Figure 8. Effect of volume fraction index *n* on the transient response of SS-FG cylindrical panels.

increase with the increase of curvature ratios$^{(R/a)}$. However, this effect is comparatively less when the R/a ratio exceeds 50. By comparing the results of cylindrical and spherical shells from Figures. 5 and 6, it is also observed that spherical shell panels (Figure. 6) have more stiffness than cylindrical panels (Figure 5), as evident from the higher frequency and lower vibration amplitude of the transient response curves of Figures 5 and 6. Moreover, it is also observed from Figures 5 and 6 that the frequency of the transient response decreases with the increase of R/a. This is due to the degradation in the shell stiffness with the increase of R/a, as mentioned above.

Figures 7 and 8 present the variation of transient displacement with time for simply supported cylindrical and spherical shells, respectively, for different values of

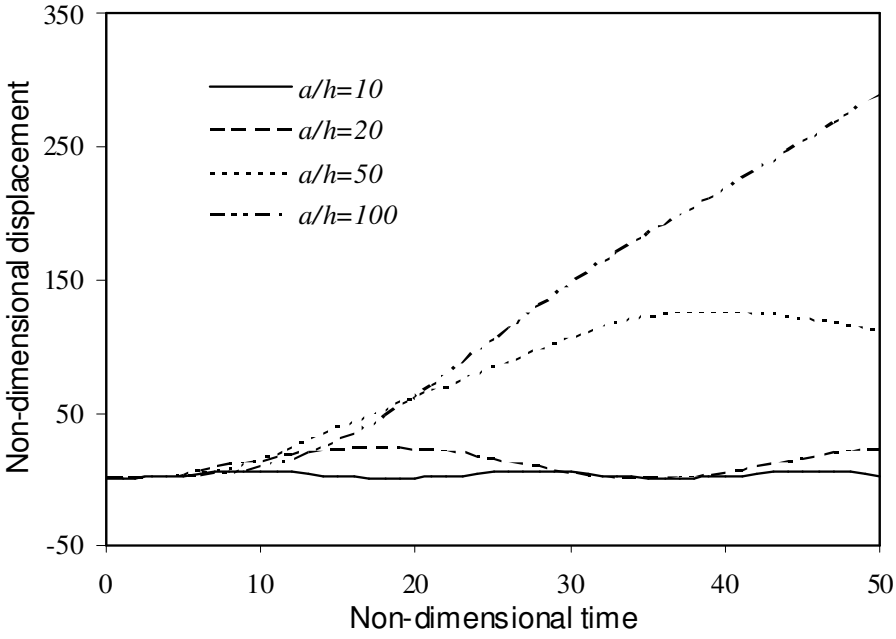

Figure 9. Effect of a/h ratios on the transient response of SS-FG cylindrical panels.

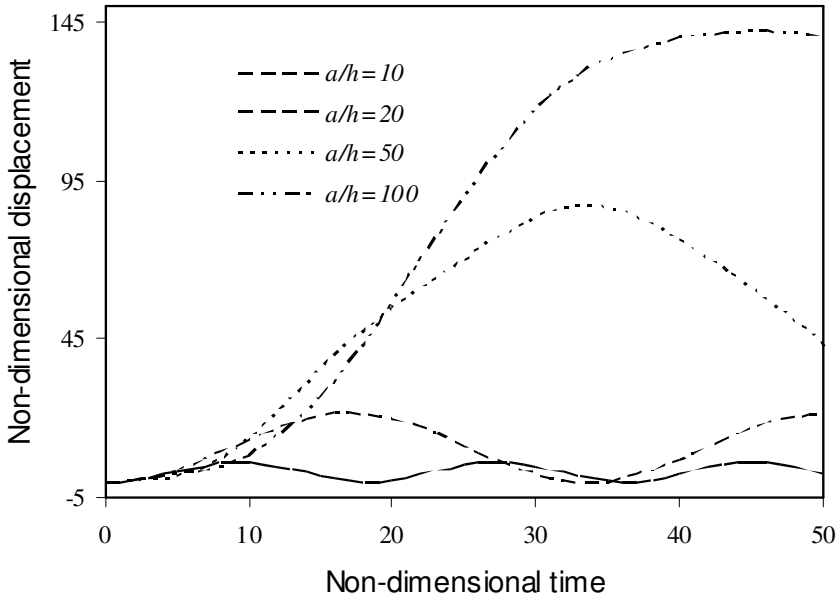

Figure 10. Effect of a/h ratios on the transient response of SS-FG spherical panels.

volume fraction index n keeping the other parameters as constant ($a/b=1$, $R/a=10$ and $a/h=20$). The amplitude of vibration increases as n increases, being the maximum for the metallic shells ($n=\infty$) and the minimum for the ceramic shells ($n=0$). It is due to the fact that Aluminum (metal) has a much lower value of the Young's modulus than that of Zirconia (ceramic).

The effect of thickness on the nonlinear transient central displacements of the FGM cylindrical and spherical shell panels for different a/h ratios is shown in Figures 9 and 10 respectively. Other parameters ($a/b=1$, $R/a=10$ and n = 1) are kept constant. It is observed from Figures 9 and 10 that the transient displacements increase and the response frequencies

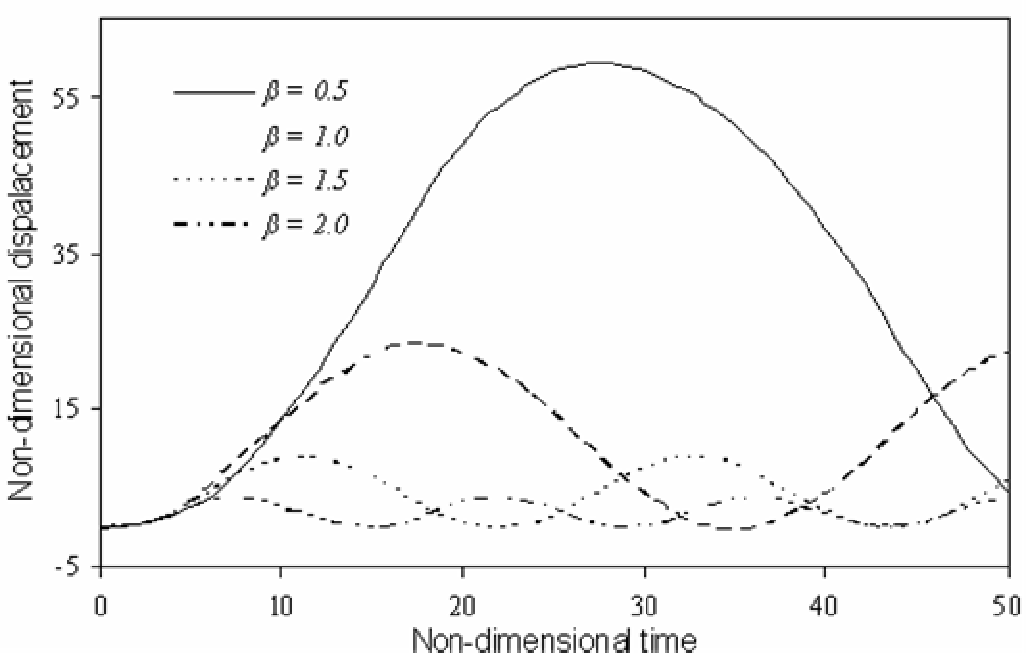

Figure 11. Effect of a/h ratios on the transient response of SS-FG spherical panels.

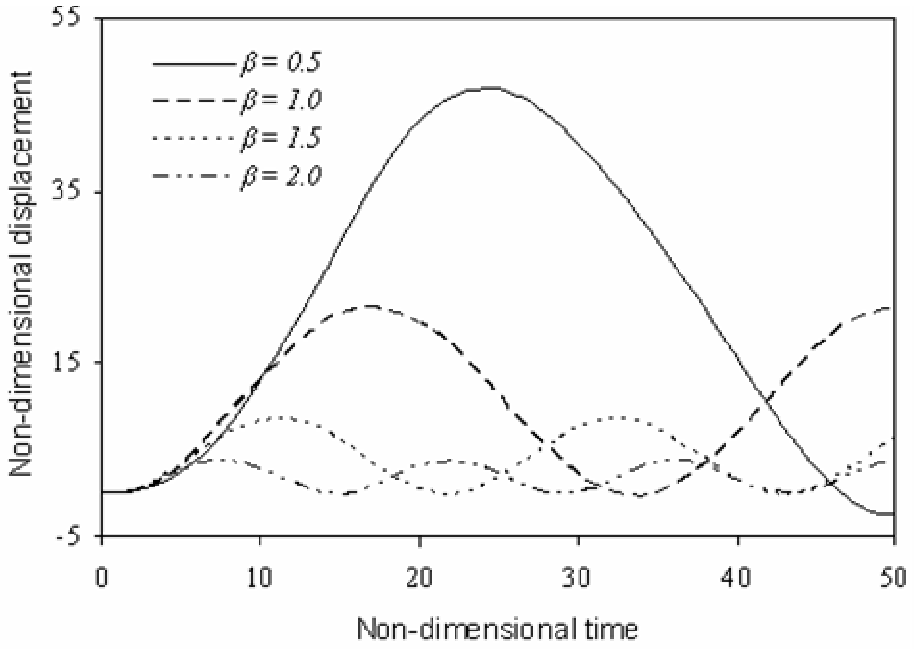

Figure 12. Effect of shell aspect ratios (β = *a/b*) on the transient response of SS-FG spherical panels.

decrease with the increase in a/h ratio. Figures 11 and 12 show the effect of shell aspect ratio (β = *a/b*) on the transient response of simply supported FGM cylindrical and spherical shells subjected to uniformly distributed load, keeping the other parameters unchanged ($R/a = 10$, *a/h* = 20 and *n* = 1). The displacements are reduced while the response frequencies are increased as β (= *a/b*) increases from 0.5 to 2.

Figures 13 and 14 present the variation of displacement with time for FGM cylindrical and spherical

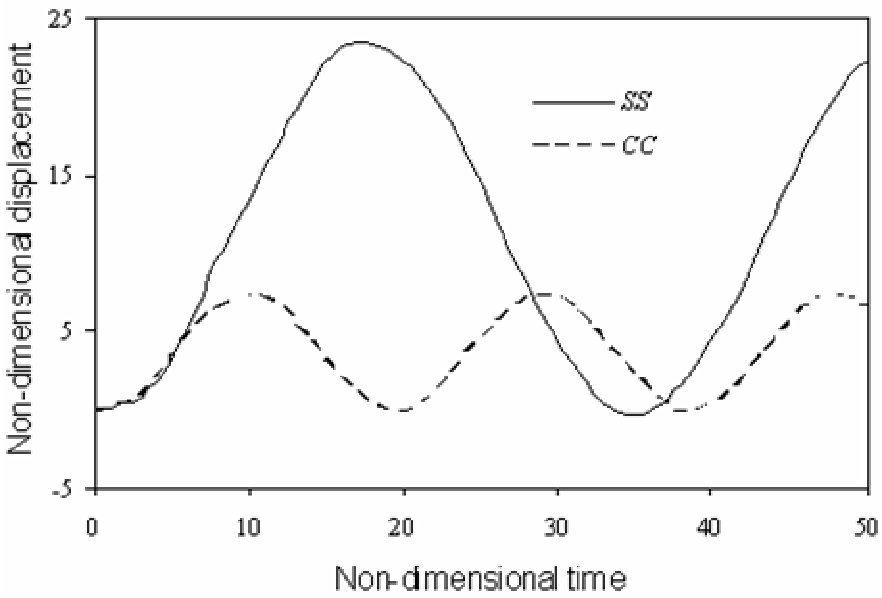

Figure 13. Effect of boundary conditions on the transient response of cylindrical FG panels.

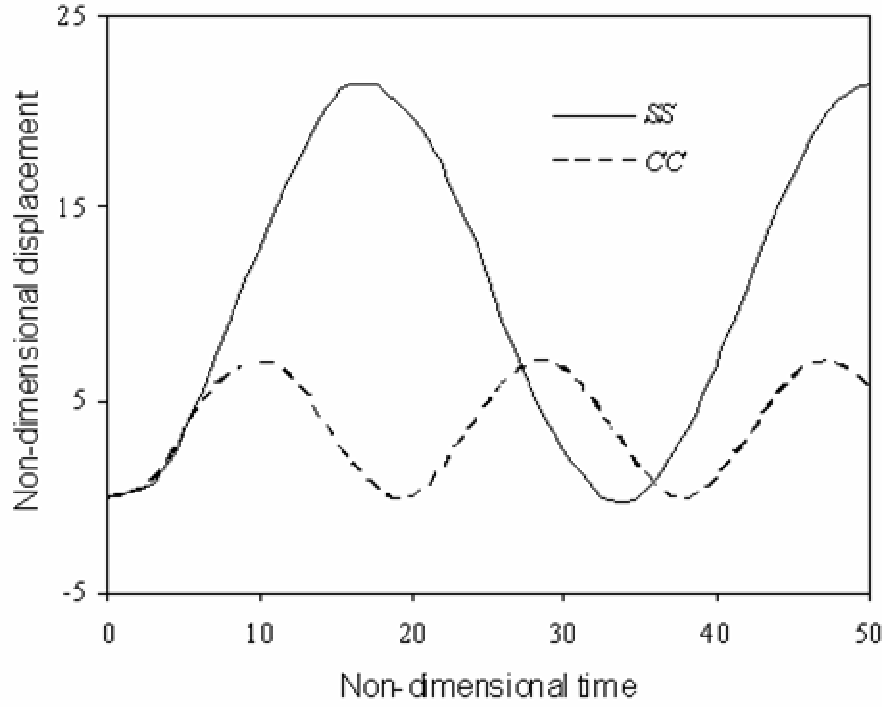

Figure 14. Effect of boundary conditions on the transient response of spherical FG panels.

shells, respectively, considering clamped and simply supported boundary conditions and keeping the remaining geometrical and material parameters as constants ($R/a=10$, *a/h* = 20, *a/b* = 1 and *n* = 1). It is clearly seen that the displacements of clamped shells are much lower than those of the simply supported shells since the effective stiffness of the clamped shell is higher than that of the simply supported shell.

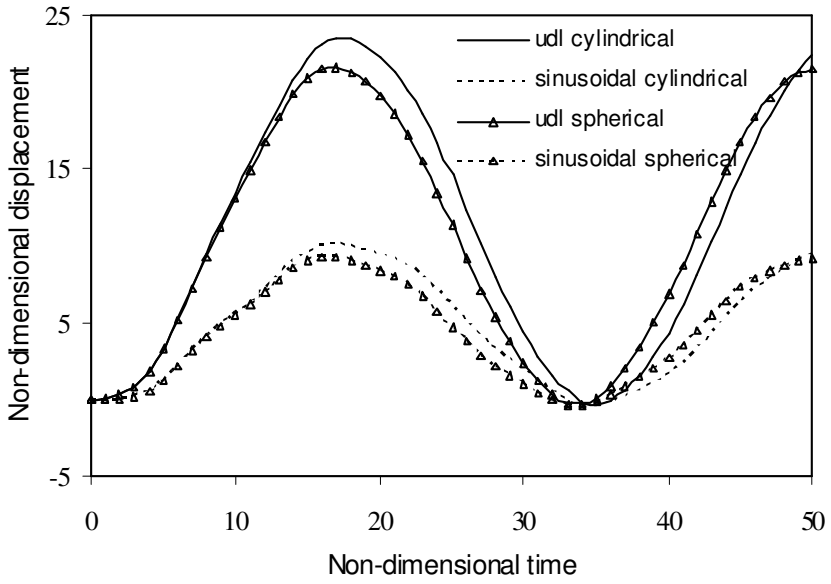

Figure 15. Effect of boundary conditions on the transient response of cylindrical FG panels.

Finally, the effect type of loadings on the nonlinear transient behavior of simply supported FGM cylindrical and spherical shell panels is studied. Here, two types of loading, uniformly distributed (*udl*, $q = q_0$) and sinusoidal loads ($q = q_0 \sin(\pi x/a)\sin(\pi y/b)$) are applied on shell panels whose geometric and elastic properties are given by *a/b*=1, $R/a = 10$, *a/h* = 20 and *n* = 1. Figure 15 shows the variation of transient displacement with time. It is evident from Figure 15 that both spherical and cylindrical shell panels with uniformly distributed load has higher transient displacement than that when subjected to sinusoidal load maintaining the same load intensity.

Conclusion

The nonlinear transient behavior of FG shell panels is investigated by using a higher-order finite element formulation. The finite element formulation developed here is validated from the good agreement of the authors' results for plate and shell problems with those of earlier investtigators from the published literature (Figures. 3 and 4). Numerical results show that the dynamic responses are significantly influenced by shell curvature, volume fraction index, thickness ratio, aspect ratio, boundary conditions and loadings.

REFERENCES

Aboudi J, Pindera MJ, Arnold SM (1999). Higher-order theory for functionally graded materials. Compos. Part B: Eng. 30: 777-832.

Allahverdizadeh A, Naei MH, Nikkhah Bahrami M (2008). Nonlinear free and forced vibration analysis of thin circular functionally graded plates. J. Sound Vib. 310: 966-984.

Bathe KJ, Ramm E, Wilson EL (1975). Finite element formulations for large deformation dynamic analysis. Int. J. Numer. Methods Eng. 9: 353-386.

Bhangale RK, Ganesan N (2006). Static analysis of simply supported functionally graded and layered magneto-electro-elastic plates. Int. J. Solids Struct. 43: 3230-3253.

Chandrashekhara K (1989). Free vibrations of anisotropic laminated doubly curved shells, Compos. Struct. 33(2): 435-440.

Civalek Ö (2006). Harmonic Differential Quadrature-finite differences coupled approaches for geometrically nonlinear static and dynamic analysis of rectangular plates on elastic foundation, J. Sound Vib. 294: 966-980.

Civalek Ö, Ülker M (2005). HDQ-FD integrated methodology for nonlinear static and dynamic response of doubly curved shallow shells, Int. J. Struct. Eng. Mechanics, 19(5): 535-550.

Fuchiyama T, Noda N (1995). Analysis of thermal stress in a plate of functionally graded material. JSAE Rev. 16: 263-268.

Fukui Y, Yamanaka N (1992). Elastic analysis for thick-walled tubes of functionally graded material subjected to internal pressure. JSME Int. J. Series 1: Solid Mechanics, Strength Mater. 35: 379-385.

GhannadPour SAM, Alinia MM (2006). Large deflection behavior of functionally graded plates under pressure loads. Compos. Struct. 75: 67-71.

Han X, Xu D, Liu GR (2002). Transient responses in a functionally graded cylindrical shell to a point load. J. Sound Vib. 251(5): 783-805.

Huang XL, Shen HS (2004). Nonlinear vibration and dynamic response of functionally graded plates in thermal environments. Int. J. Solids Struct. 41: 2403-2427.

Kant T, Khare RK (1997). A higher-order facet quadrilateral composite shell element, International J. Numer. Methods Eng. 40: 4477-4499.

Koizumi M (1993). Concept of FGM. Ceramic Trans. 34: 3-10.

Loy CT, Lam KY, Reddy JN (1999). Vibration of functionally graded cylindrical shells. Int. J. Solids Struct. 41: 309-324.

Naidu NVS, Sinha PK (2006). Nonlinear transient analysis of laminated composite shells in hygrothermal environments. Compos. Struct. 72: 280-288.

Nath Y, Dumir PC, Bhatia RS, (1985). Nonlinear static and dynamic analysis of circular plates and shallow spherical shells using the

collocation method. Int. J. Numer. methods in Eng. 21:565-578.
Ng TY, Lam KY, Liew KM. (2000). Effects of FGM materials on the parametric resonance of plate struct. Comput. Methods Appl. Mech. Eng. 190: 953-962.
Panda S, Ray MC (2006). Nonlinear analysis of smart functionally graded plates integrated with a layer of piezoelectric fiber reinforced composite. Smart Mater. Struct. 15: 1595-1604.
Patel BP, Gupta SS, Loknath MS, Kadu CP (2005). Free vibration analysis of functionally graded elliptical cylindrical shells using higher-order theory. Compos. Struct. 69: 259-270.
Pradhan SC, Loy CT, Lam KY, Reddy JN (2000). Vibration characteristics of functionally graded cylindrical shells under various boundary conditions. Appl. Acoustics, 61: 111-129.
Praveen GN, Chin CD, Reddy JN (1999). Thermoelastic analysis of functionally graded ceramic-metal cylinder. J. Eng. Mechanics, 125 (11): 1259-1267.
Praveen GN, Reddy JN (1998). Nonlinear transient thermoelastic analysis of functionally graded ceramic-metal plates. Int. J. Solids Struct. 35: 4457-4476.
Ray MC, Sachade HM (2006). Exact solutions for the functionally graded plates integrated with a layer of piezoelectric fiber-reinforced composite. ASME J. Appl. Mech. 73: 622-632.
Reddy JN (1984). Exact solutions of moderately thick laminated shells. ASCE J. Appl. Mech., 110(5): 794-809.
Reddy JN (2000). Analysis of functionally graded plates. Int. J. Numer. Methods Eng. 47: 663-684.
Reddy JN (2003). Mechanics of laminated plates and shells. CRC Press, Boca Raton.
Shen HS (2002). Nonlinear bending response of functionally graded plates subjected to transverse loads and in thermal environments. Int. J. Mech. Sci. 44: 561-584.
Wetherhold RC, Seelman S, Wang J (1996). The use of functionally graded materials to eliminate or control thermal deformation. Composite Sci. Technol. 56:1099-1104.
Woo J, Meguid SA (2001). Nonlinear analysis of functionally graded plates and shallow shells. Int. J. Solids Struct. 38:7409-7421.
Woo J, Meguid SA, Ong LS (2006). Nonlinear free vibration behavior of functionally graded plates. J. Sound Vibration, 289:595-611.
Yang J, Kitipornchai S, Liew KM (2003). Large amplitude vibration of thermo-electro-mechanically stressed FGM laminated plates. Comput. Methods Appl. Mech. Eng. 192: 3861-3885.
Yang J, Shen HS (2002). Vibration characteristics and transient response of shear-deformable functionally graded plates in thermal environments. J. Sound Vib. 255: 579-602.
Yang J, Shen HS (2003). Free vibration and parametric resonance of shear deformable functionally graded cylindrical panels. J. Sound Vib. 261:871-893.